Published in final edited form as:
Biosens Bioelectron. 2013 August 15; 46: 183–189. doi:10.1016/j.bios.2013.02.030.

Glycosylated aniline polymer sensor: Amine to imine conversion on protein–carbohydrate binding

Zhe Wang[a], **Chunyan Sun**[a,b], **Giri Vegesna**[c], **Haiying Liu**[c], **Yang Liu**[d], **Jinghong Li**[d], and **Xiangqun Zeng**[a,*]

[a] Department of Chemistry, Oakland University, Rochester, MI 48309, United States

[b] Department of Food Quality and Safety, Jilin University, Changchun 130062, PR China

[c] Department of Chemistry, Michigan Technological University, Houghton, MI 49931, United States

[d] Department of Chemistry, Tsinghua University, Beijing 100084, PR China

Abstract

In this report, functionalized mannosylated aniline polymer (manno-PANI) was investigated as an electrochemical platform to study carbohydrate–protein interactions by exploiting the conductivity change of manno-PANI when the specific lectin binding occurs. A systematic study was performed to characterize the interconversion of polyaniline content (from amine to imine) in manno-PANI by UV–vis spectroscopy during its binding with concanavalin A (Con A). Both X-ray photoelectron spectrometry (XPS) and UV–vis results suggest that Con A binding with the manno-PANI film triggers the switching of amine functionalities in the polyaniline backbone, converting them to imine forms. Electrochemical impedance spectroscopy (EIS) was used to quantify the specific interactions between Con A and mannose by measuring the impedance change of manno-PANI film for the detection of Con A. A linear relationship between the impedance and Con A concentration was obtained, and the detection limit reaches to 0.12 nM Con A in a buffer solution (pH=7.4), whereas the addition of nonspecific control lectins to the same manno-PANI film gave very little impedance variations. Stability characterization of the manno-PANI film over 20 weeks shows a maximum drift of only 3% from the original signal. Thus, the uniquely constructed carbohydrate–PANI hybrid is a promising new carbohydrate recognition moiety for studying carbohydrate-protein interactions, presumably leading to a new electrochemical method for characterization of carbohydrate–protein interactions and carbohydrate-mediated intercellular recognitions.

Keywords

Polyaniline; Carbohydrate; Electrochemical biosensor; Glycosylated aniline; EIS; Biorecognition

1. Introduction

Carbohydrate–protein interactions are abundant in many biological processes including cell–cell communication, signal transduction, host–pathogen recognition, inflammation and

* Corresponding author. Tel.: +1 248 370 2881; fax: +1 248 370 2321. zeng@oakland.edu (X. Zeng)..

Appendix A. Supporting information

Supplementary data associated with this article can be found in the online version at http://dx.doi.org/10.1016/j.bios.2013.02.030.

tumor cell metastasis (Bertozzi and Kiessling, 2001; Lis and Sharon, 1998; Manning et al., 1995; Plante et al., 2001; Shaanan et al., 1991; Sharon and Lis, 1986). When compared to DNA–protein and protein–protein interactions, the carbohydrate–protein interactions are harder to measure due to the lack of chromophores in carbohydrate structures and the presence of multitudes of different carbohydrate monomers, stereoisomers and their combination possibilities. In recent years, advances in the fields of carbohydrate biointerface developments have made available a great number of innovative carbohydrate biosensors for characterizing carbohydrate–protein interactions. The most promising approach is to create sensory materials not only containing the carbohydrate receptors for efficient binding with target proteins but also bearing perturbable functionalities for sensitive transduction of recognition events.(Loaiza et al., 2011; Pu et al., 2010; Szunerits et al., 2010) Numerous carbohydrate biosensors were reported by incorporating molecular labels such as fluorophores or biotin either into carbohydrate moiety or protein moiety for detection.(Chen et al., 2012; Gruber et al., 2011; Jelinek and Kolusheva, 2004) Fluorescence or biotin labeling requires additional steps. Labeling a biomolecule can drastically change its binding properties and label can also interfere with the true binding process.(Haab, 2003) label-free carbohydrate biosensors in which the binding of carbohydrate with the protein is transduced to a signal that can be measured directly have been demonstrated including dual polarization interferometry (Ricard-Blum et al., 2006), quartz crystal microbalance (Pei et al., 2007; Shen et al., 2007b), surface plasmon resonance (Munoz et al., 2009; Murthy et al., 2006, 2012), electrochemical voltammetry (Dai et al., 2006; He et al., 2011), NMR(Mayer and Meyer, 2001) and isothermal titration calorimetry (Doyle, 1997). However, non-specific interactions such as physical adsorption are serious problems for the label-free carbohydrate biosensors since carbohydrate–protein interactions are typically weaker than protein–protein interactions which often leads to small signal to noise ratio and low sensitivity of the measurements.

Electrochemical methods such as cyclic voltammetry (CV) and electrochemical impedance spectroscopy (EIS) have the capability of measure the weak carbohydrate-protein interactions.(Bogomolova et al., 2009; Ding et al., 2009; Yu et al., 2006) By using electrochemical probes either conjugated to the carbohydrate moiety or added into the testing solution, they provide a unique electrochemical platform for quantifying carbohydrate–protein interactions.(Zhou et al., 2011) For example, Hu et al. (2012) reported an electrochemical biosensor using polyaniline and sugar composites as recognition elements. In their method, aniline was chemically polymerized on the surfaces of carbon nanotubes and D-glucose was modified on the carbon nanotube–polyaniline nanocomposites via Schiff-base reaction subsequently. The use of polyaniline as an electrochemical reporter moiety is elegant, however the conjugation of glucose to polyaniline using Schiff-base reaction could lead to an open ring reaction and the product of Schiff-base reaction is very sensitive to pH (e.g. lower pH can result in decomposition of the product). The lack of control of polyaniline and sugar conjugation via Schiff-base reaction and the use of $K_3Fe(CN)_6/K_4Fe(CN)_6$ redox probe in EIS sensing made this method less practical. Szunerits et al. (2010) characterized the carbohydrate and its complementary lectin binding using EIS by directly coupled carbohydrate to the boron-doped diamond electrode terminated with alkynyl functional group via copper (I) catalyzed azide alkyne cycloaddition click reaction. This carbohydrate biointerface fabrication still requires several steps and the amount of carbohydrate receptors incorporated is monolayer which may limit its sensitivity and dynamic range.

Here we report a new and better electrochemical based label free carbohydrate biosensor in which a well-defined aniline monomer bearing α-mannoside residue at *ortho*-position of the aniline ring enables for one-step electrochemical polymerization of the glycosylated aniline polymer (manno-PANI) on the electrode substrate with controlled thickness and porosity

(Scheme 1 and Scheme S1). The glycosylated aniline polymer was shown to maintain the bioactivity of the natural sugar and can directly transduce the carbohydrate–protein binding to a change of the electrical signal (impedance by EIS or current by CV) due to the extremely sensitivity of the polyaniline to its protonation/deprotonation states (Scheme 1). Multiple techniques including X-ray photoelectron spectroscopy (XPS), scanning electron microscopy (SEM), UV–vis spectroscopy, CV have been used to characterize the electrochemical polymerization of the glycosylated aniline and its electrochemical properties. Quantitative characterization of analytical parameters of the manno-PANI as a biosensor for detection of Con A by EIS shows high sensitivity, selectivity and stability validating its use as a new carbohydrate recognition moiety for studying carbohydrate-protein interaction and for label free carbohydrate based biosensor development.

2. Materials and methods

2.1. Materials

Indium tin oxide (ITO) glass slides (CD-501N-CUV) were purchased from Delta Technologies Co. Ltd. Concanavalin A (Con A), peanut agglutinin (PNA), Elderberry lectin (SNA), *Ulex europaeus* agglutinin (UEA), Wheat germ agglutinin (WGA), *Pisum sativum* agglutinin (PSA) were purchase from Sigma-Aldrich or FluoProbes®/Interchim Co. Ltd. All reagents and material were analytical grade, and solvents were purified by standard procedures. (4-(2-hydroxyethyl)-1-piperazineethanesulfonic acid) (HEPES) was purchased from Sigma-Aldrich.

2.2. Synthesis and characterization of glycosylated aniline polymer film

The manno-PANI was synthesized following a six-step method (Scheme S1) with details presented in the supplementary information. Electrochemical experiments were carried out using VersaSTAT MC (Princeton AMETEK, US) instrument. Manno-PANI was made by electrodeposition on the ITO slide as the working electrode (sensing area is 2.8 cm^2) in HEPES (pH=7.4) buffer containing 20 mM monomer of mannose functionalized aniline by cyclic voltammetry (CV). CV was performed between –0.2 V and 1.2 V versus Ag/AgCl reference electrode at 50 mV/s. Nitrogen was purged into the system to remove the oxygen in the electrolytes. Pt wire was used as the counter electrode. Before further measurements, the manno-PANI modified electrode was rinsed by HEPES to remove unbound monomer and then dried by high purity nitrogen flow. And then, the electrodes were immersed and incubated in HEPES containing different concentrations of lectins and 2 mM Ca^{2+} in variable time (from 0 min to 600 mins) for further characterizations. Con A is a homotetramer with each sub-unit (26.5 KDa, 235 amino-acids, heavily glycated). Divalent cations (usually Mn^{2+} and Ca^{2+}) must be present to permit the binding of Con A to carbohydrates because they are necessary in order to get an active Con A conformation. Ca^{2+} is used in all the lectins and manno-PANI binding experiments (Loris et al., 1998; Min et al., 1992)

The surface morphology of modified electrodes was characterized by scanning electron microscopy (SEM) (JSM-6510GS from JEOL), operating with an accelerating voltage of 20 kV. XPS spectra were obtained with a PHI 5000 VersaProbe X-ray photoelectron spectrometer. A monochromatic Al-KR X-ray source (1486.7 eV) was used. N 1 s of XPS core level spectra were acquired with a pass energy of 20 eV, a step of 0.1 eV, and a dwell time of 200 ms. The takeoff angle between the sample film surface and the photoelectron energy analyzer was 90 degree. The typical operating pressure was around 5×10^{-10} Torr in the sample chamber. The Shirley function was used as a background and Gaussian–Lorentzian cross-products were used to fit the individual peaks.(Ray et al., 1989a, 1989b; Tan et al., 1989a) UV–vis spectra of the manno-PANI modified ITO electrodes were

recorded at the open circuit potential using a Cary 100 Bio spectrophotometer (Varian). The modified ITO slides were placed in the light path so that the transmitted light passing directly through it and all spectra were calibrated by a baseline of neat ITO. EIS experiments were carried out under open circuit potential using VersaSTAT MC instrument as well. All experiments were performed at room temperature (298 K).

2.3. Formation and characterization of mannosylated aniline polymer film

Mannosylated aniline monomer was electrochemically polymerized to form manno-PANI on the ITO electrode in HEPES (pH=7.4) buffer as reported in neutral aqueous media (Chan et al., 1994; Nguyen et al., 1999; Solanki et al., 2008; Yue et al., 1991; Zhou et al., 2009). At pH (7.4), carbohydrates are uncharged and their bioactivities are maintained. The HEPES buffer contains bulky zwitterionic 4-(2-hydroxyethyl)-1-piperazineethanesulfonic acid which is deliberately chosen for several reasons. First, the bulky ion of HEPES will minimize its migration as the counter ion within the aniline polymer film for the charge compensation when mannosylated aniline monomer is electrochemically oxidized to form manno-PANI. This will result in an emeraldine (half-oxidized) manno-PANI formation rather than fully oxidized pernigraniline form. The emeraldine form of manno-PANI is beneficial for impedance-based detection of its binding with Con A for several reasons. First, it contains protonated amine functionality; second, if binding of Con A to manno-PANI can lead to the change of the manno-PANI oxidation states due to deprotonation, the bulky ions of HEPES will not be able to quickly compensate the charge, thus any change of the conductivity of the manno-PANI film can be ascribed to the lectin–carbohydrate binding events. This strategy significantly reduces the noise and increases the signal to noise ratio for sensitive detection of mannose–Con A interactions by EIS readout. Finally, HEPES buffer is better than PBS buffer in lectin binding reaction because PBS buffer can react with trace metal ions such as Ca(II) to form calcium phosphate precipitates. Similarly to other alkyl substituted aniline polymerization, the steric hindrance of the mannose substituent in aniline monomer can induce torsion angle between phenyl rings in the polymer backbone during electrochemical polymerization process. Subsequently, it reduces the π-conjugation in the polyaniline chain and destabilizes the polysemiquinone radical cation form (Wei et al., 1989). The stability of the polysemiquinone radical cation is decreased in the substituted derivatives to the extent that the reduced amine form of the polymer is directly oxidized to the imine form, and that the semiquinone form has no detectable existence under the conditions employed in the CV studies. As shown in (Fig. S1), only one pair of redox peaks located at 0.38 V and 0.25 V was observed in the CV. This result is consistent with the characteristics of substituted aniline that is partially oxidized to form the emeraldine PANI (Kilmartin and Wright, 1999; Snauwaert et al., 1987). In neutral media, PANI could grow with the same efficiency as in acidic media (Nguyen et al., 1999), although there was only one pair of redox peaks in CV (Duic and Mandic, 1992). The surface coverage of the manno-PANI is 1.71×10^{-7} mol/cm^2 calculated based on the charge from the CV curves. (Granot et al., 2005; Yin et al., 2006) Since the aniline was covalently bonding with mannose substituent in a ratio of 1:1, the total amount of sugar is about 479 nM on the ITO electrode.

3. Results and discussion

3.1. Characterization of mannosylated polyaniline film

The manno-PANI modified ITO electrodes were characterized by CV in the absence and the presence of Con A at various concentrations (Fig. 1). In the presence of Con A, both anodic and cathodic peak currents decreased. The decreased current could be ascribed to the binding of Con A to the manno-PANI. In comparison to the mannose complementary lectin Con A, the other control lectins (Fig. S2) gave much less current decrease due to non-

specific interactions. The binding of Con A to the manno-PANI could increase the interchain distance of the polymer chains and partially block the electron-transfer process among the manno-PANI (Lis and Sharon, 1998), (Ervin et al., 2009; Lathrop et al., 2010; White et al., 2007) from half oxidized emeraldine state to the fully oxidized pernigraniline state. Since the counterion is very big, we can neglect the counterion transfer to the manno-PANI and attribute the changes of the conductivity of manno-PANI to Con A binding only. Interestingly, a positive shift of anodic peak potential is observed with the increase of Con A concentrations but no potential shift for cathodic peak is observed. We rationalize that the initiate state of polyaniline is emeraldine form, and parts of emeraldine were oxidized after its binding to Con A. This rationalization was further supported by in-situ UV–vis absorption spectra and XPS results below.

Surface morphology of manno-PANI was investigated by SEM. Fig. 2 (a) shows the SEM image of manno-PANI on the ITO electrode. The electrochemically synthesized manno-PANI shows a textile structure which is different from the flower-like morphology observed in unsubstituted polyaniline films (Sazou, 2001; Yavuz et al., 2010). This is consistent with the CV results in Fig. S1 that the steric hindrance of glycosylated aniline monomer affects polymerization of aniline. As shown in Fig. 2(a), the white spots on the surface are likely due to the electron aggregation at mannose functional groups. Fig. 2(b) shows that after the manno-PANI film was treated with Con A solution, the manno-PANI film morphology changed to a sponge-like architecture, suggesting a complete binding of manno-PANI to Con A. We verified the presence of Con A by further adding *Escherichia coli* W1485 (Fig. 2c) since the lipopolysaccharides (LPS) of the O-antigen of *E. coli* W1485 have glucose subunit which can bind selectively with Con A. (Lis and Sharon, 1986; Otto et al., 1999; Shen et al., 2007b). As shown in Fig. 2(c) and (d), *E. coli* bacteria were observed as uniformly distributed on the manno-PANI–Con A film, further proving the specificity of binding between manno-PANI and Con A.

3.2. Analysis of Con A binding process by UV–vis absorption spectroscopy

The manno-PANI and its interaction with Con A were characterized by the UV–vis absorption spectroscopy (Fig. 3). Consistent with the interpretation of electrochemical CV study in Figs. 1 and 2, the manno-PANI in the absence of Con A shows two absorbance maxima at 325 nm and 563 nm respectively. These are the characteristics of emeraldine form of PANI. The binding of Con A to the manno-PANI causes an increase of absorbance band at 442 nm (polaron) and the decreases of the absorbance bands at 325 nm (π–π* transition) and 563 nm (bipolaron (doped)). The isosbestic point (Masters et al., 1991) at 510 nm confirms that the emeraldine form of manno-PANI changes to the pernigraniline form of PANI when sufficient Con A has been added (Albuquerque et al., 2000; Masters et al., 1991). This phenomenon also was shown in the absorption spectra of polyaniline and substituted polyaniline when the pH was changed from low (two) to high (nine) (Ayad et al., 2010; Lindfors and Ivaska, 2002). The possibility of degradation of manno-PANI is unlikely since there is no new absorption band emerging (Libert et al., 1997). The UV–vis absorption spectra of manno-PANI binding to Con A shows the same trends as substituted PANI when the pH is increased from 2 to 9, suggesting that binding of Con A to manno-PANI leads to deprotonation of manno-PANI from emeraldine state to pernigraniline state. Carbohydrates are weak acids with pKa values ranging from 12 to 14 (e.g. galactose 12.39, glucose 12.28, xylose 12.15, mannose 12.08 and fructose 12.03). Thus, carbohydrate–protein interaction would be sensitive to local pH change. The binding of a carbohydrate to a protein often involves a subtle conformational change of protein that can result in the protonation/deprotonation of the protein (Zand et al., 1971). In the presence of metal ion (Mn^{2+}, Ca^{2+}), ion and proton exchange could affect the binding of carbohydrate to the protein (Appenzeller-Herzog et al., 2004; Iobst et al., 1994). As shown in Scheme 1, if the proton

switching occurs during the binding of carbohydrate to protein, it will lead to changes of local charge distribution of the polyaniline (Focke et al., 1987),(Chen et al., 2012). We further characterized the oxidation state of manno-PANI with and without Con A binding by XPS study below (Fig. 4).

3.3. Characterization of the energy level of the nitrogen elements in polyaniline by XPS

XPS was used to characterize the change of chemical composition of manno-PANI upon its binding to Con A. The XPS was used to analyze quantitatively the nitrogen oxidation states to understand the chemical microenvironment change of manno-PANI when it binds to Con A. Typically the protonation occurs preferentially at the imine sites of PANI chain (MacDiarmid et al., 1987). Fig. 4 shows the N1s XPS spectra of manno-PANI before and after interactions with Con A. It is worth noting that the signal consists of three components corresponding to three different nitrogen species, i.e. imine, amine and radical cationic nitrogen respectively after deconvolution of the XPS spectra (Muilenberg, 1997). The one centered at 398.8 eV is attributed to the protonated nitrogen atom (–NH–) coming from the amine group in the emeraldine form.(Lim et al., 1998; Tan et al., 1989a; Yue and Epstein, 1991) Typically the binding energy of amine nitrogen (–NH–) in polyaniline is higher than 399.0 eV. (Lim et al., 1998; Tan et al., 1989a; Yue and Epstein, 1991) The reduced binding energy of nitrogen in –NH– of manno-PANI is likely due to the mannose substituents (Choudary et al., 2006). The binding energy of imine nitrogen (–N=) as a result of amine deprotonation in the quinone structure of manno-PANI is at 398.0 eV. There is also some signals above 399.5 eV expected from the higher oxidization state of nitrogen element, (the radical cationic nitrogen –N•$^{+}$–) in the film (Shen et al., 2007a; Tan et al., 1989b; Yue and Epstein, 1991). It is –N•$^{+}$–, which results from the protonation of the quinonoid imine in the ionic environment.(Ray et al., 1989a, 1989b; Yue and Epstein, 1991) As shown in Fig. 4b, after interactions with Con A, the nitrogen binding energy peaks of manno-PANI shift to lower binding energy states. In manno-PANI, the atomic concentrations of amine (–NH–) account for about 58.6% and imine accounts of 18.3%. After interactions with Con A, content of protonated nitrogen (–NH–) decreased to 17.6% and the imine nitrogen (–N=) increases to 67.5%. The content of the radical cationic nitrogen also decreased from 23.1% to 14.9%. It confirms that most of emeraldine has been converted to pernigraniline on PANI skeleton. In the protonated form of manno-PANI, emeraldine form of polyaniline has highest conductivity among various oxidation states of PANI (vanderSanden, 1997), since the free doublet electrons on the nitrogen atoms participate in the formation of orbitals delocalized along the polymer chain. However quinoid form is unstable in non-ionized state. Pernigraniline shows very low conductivity due to the lack of disorder in PANI. A marginal degree of protonation is sufficient to induce the conductor-insulator transition upon Con A binding.

In summary, the significant morphological and spectral change of manno-PANI observed by SEM images and UV–vis absorption spectra, respectively and the changes of nitrogen binding energy upon addition of Con A support that trace amount of Con A binding to mannose residues in the manno-PANI can significantly trigger polyaniline electronic microenvironment changes which can be used for the sensitive detection of specific carbohydrate-protein interaction at very low protein concentration.

3.4. Quantification of mannosylated polyaniline–protein interactions by electrochemical techniques for sensor application

In EIS, the electrode–solution interface is perturbed with an alternating signal of very small magnitude, thus, EIS can be considered non-invasive for measurements of the conductivity change. Fig. 5a shows the Bode plot of manno-PANI at various Con A concentrations. The

electrochemical impedance–frequency plot (Bode plot) is more practical to apply in sensor system.

The formation of manno-PANI increased the substrate ITO impedance to 5000Ω at 1 Hz. This impedance is higher than pure PANI film reported in the literature since the conjugated structure and doping mode of PANI was influenced by substituted group. When Con A was added to the manno-PANI modified ITO electrode, the resulting impedance increased remarkably. As it is reported that the peripheric protein surface adjacent to the carbohydrate recognition domain (CDR) of natural lectins may interact with hydrophobic groups, the increase of impedance could be attributed to the structure of polyani-line change caused by binding of Con A to the mannose in the presence of Ca^{2+} ions. The Con A–mannose interactions result in partial deprotonation of polyaniline so that the content of imine functionality increases but quinoid form decreases. This changes the disorder in PANI, which shows higher conductivity at emeraldine form typically. As shown in Fig. 5a, the increase of impedance of manno-PANI modified electrode is Con A concentration-dependent in the range of 3–15 nM with the following linear relationship.

$$\mathrm{Z}_{\mathrm{Impedance\ at\ 1Hz}}\,(\mathrm{KOhm}) = 24.3 \times \mathrm{C}_{\mathrm{ConA\ concentration}}\,(\mathrm{nM}) - 8.08 \left(r^2 = 0.995\right)$$

The detection limit was calculated to be 0.12 nM (S/σ=3, where s is the standard deviation of the impedance obtained in the absence of Con A), which is the lowest detection limits when compared with those reported in the literature.

Additionally, in order to further ascertain the specificity of Con A and manno-PANI interactions, a panel of negative control lectins including PNA (galactose/*N*-acetylgalactosamine binding lectin), SNA (*N*-acetylneuraminic acid binding lectin), UEA (Fucose binding lectin), WGA (*N*-acetylglucosamine binding lectin), PSA (mannose binding lectin) that are known to specifically recognize other natural monosaccharide subunits were assayed in the same conditions via EIS readout (Fig. 5b). In stark contrast, when nonspecific lectins with the concentration of 6 nM were added to the manno-PANI film, very small impedance changes were observed. Without specific mannose–lectin interactions, the structure of manno-PANI remained intact and conductivity is a constant. The slight signal change is explained as the non-specific adsorptions of control lectins on the manno-PANI surface. These data have successfully demonstrated the feasibility of the uniquely glycosylated polyaniline biofilm containing natural saccharide for the accurate probing of specific carbohydrate–protein interactions via measurement of the conductivity changes of glycosylated aniline polymer.

The manno-PANI modified electrode has a very good long-term stability characterized by EIS and UV–vis experiments. In Fig. S3 and Table S1, the impedance values at 1 Hz and absorbance values at 560 nm towards the same concentration of Con A were plotted over the measurement period of 20 weeks. The signal drift is normalized to the first measurement of sensor response on the first day. The reported values are the result of averaging at least three measurements. A maximum drift of 3% in EIS measurement was observed in these 20 weeks highlighting the stability of the manno-PANI films for practical applications.

4. Conclusion

We have demonstrated that glycosylated aniline polymer can be used as an effective new biomaterial for label free electrochemical characterization of carbohydrate–protein interactions based on the extremely high sensitivity of manno-PANI to the local proton exchange. The deprotonation of manno-PANI caused by specific interactions between

lectins and carbohydrates on the manno-PANI resulted in the switching of amine to imine in the manno-PANI supported by UV–vis absorption and XPS characterization. As a result of this conversion in manno-PANI, the conductivities of film were dramatically decreased upon binding with Con A with detection limits of 1.2 nM and a linear range of 3–15 nM. There is little signal changes in the presence of nonspecific lectins during the EIS measurement. This confirms the extreme sensitivity and selectively of manno-PANI to the specific lectin binding. The simplicity of synthesis of glycosylated aniline monomer, the versatility of polymerization of the glycosylated aniline by chemical or electrochemical oxidation, and the sensitivity of the EIS readout without using redox probes render this method feasible for various carbohydrate array fabrication and miniaturization. Thus the glycosylated aniline polymer can be used to facilitate the better understanding of the "glycomics" as well as the development of early-state disease diagnosis using carbohydrate biosensors.

Supplementary Material

Refer to Web version on PubMed Central for supplementary material.

Acknowledgments

Zeng X. would like to acknowledge the partly support by NIH R21, Oakland University Research Excellence funds and National Natural Science Foundation of China (No. 21128005). Chunyan Sun likes to acknowledge the funds from China Scholarship Council for her visit at Oakland University. Authors would like to thank Professor Fen-Tair Luo to assist for Mass spectroscopic characterization of products and Professor Qian Zhou of Mechanical Engineering Department to assist for XPS instrument operation. SEM instrument is funded by NSF (the award number 1040304). H. Liu would like to acknowledge the NSF support.

References

Albuquerque JE, Mattoso LHC, Balogh DT, Faria RM, Masters JG, MacDiarmid AG. Synthetic Metals. 2000; 113(1-2):19–22.

Appenzeller-Herzog C, Roche AC, Nufer O, Hauri HP. The Journal of Biological Chemistry. 2004; 279(13):12943–12950. [PubMed: 14718532]

Ayad MM, Salahuddin NA, Alghaysh MO, Issa RM. Current Applied Physics. 2010; 10(1):235–240.

Bertozzi CR, Kiessling LL. Science. 2001; 291(5512):2357–2364. [PubMed: 11269316]

Bogomolova A, Komarova E, Reber K, Gerasimov T, Yavuz O, Bhatt S, Aldissi M. Analytical Chemistry. 2009; 81(10):3944–3949. [PubMed: 19364089]

Chan HSO, Ng SC, Ho PKH. Macromolecules. 1994; 27(8):2159–2164.

Chen YN, Vedala H, Kotchey GP, Audfray A, Cecioni S, Imberty A, Vidal S, Star A. Acs Nano. 2012; 6(1):760–770. [PubMed: 22136380]

Choudary BM, Roy M, Roy S, Kantam ML, Sreedhar B, Kumar KV. Advanced Synthesis & Catalysis. 2006; 348(12-13):1734–1742.

Dai Z, Kawde A-N, Xiang Y, La Belle JT, Gerlach J, Bhavanandan VP, Joshi L, Wang J. Journal of American Chemical Society. 2006; 128(31):10018–10019.

Ding L, Cheng W, Wang XJ, Xue YD, Lei JP, Yin YB, Ju HX. Chemical Communications. 2009; 46:7161–7163. [PubMed: 19921016]

Doyle ML. Current Opinion in Biotechnology. 1997; 8(1):31–35. [PubMed: 9013658]

Duic L, Mandic Z. Journal of Electroanalytical Chemistry. 1992; 335(1-2):207–221.

Ervin EN, White RJ, White HS. Analytical Chemistry. 2009; 81(2):533–537. [PubMed: 19140775]

Focke WW, Wnek GE, Wei Y. Journal of Physical Chemistry-Us. 1987; 91(22):5813–5818.

Granot E, Katz E, Basnar B, Willner I. Chemistry of Materials. 2005; 17(18):4600–4609.

Gruber K, Horlacher T, Castelli R, Mader A, Seeberger PH, Hermann BA. Acs Nano. 2011; 5(5): 3670–3678. [PubMed: 21388220]

Haab BB. PROTEOMICS. 2003; 3(11):2116–2122. [PubMed: 14595810]

He XP, Wang XW, Jin XP, Zhou H, Shi XX, Chen GR, Long YT. Journal of American Chemical Society. 2011; 133(10):3649–3657.

Hu F, Chen S, Wang C, Yuan R, Xiang Y, Wang C. Biosensors and Bioelectronics. 2012; 34(1):202–207. [PubMed: 22387041]

Iobst ST, Wormald MR, Weis WI, Dwek RA, Drickamer K. The Journal of Biological Chemistry. 1994; 269(22):15505–15511. [PubMed: 8195194]

Jelinek R, Kolusheva S. Chemical Reviews. 2004; 104(12):5987–6015. [PubMed: 15584694]

Kilmartin PA, Wright GA. Synthetic Metals. 1999; 104(3):145–156.

Lathrop DK, Ervin EN, Barrall GA, Keehan MG, Kawano R, Krupka MA, White HS, Hibbs AH. Journal of American Chemical Society. 2010; 132(6):1878–1885.

Libert J, Cornil J, dosSantos DA, Bredas JL. Physical Review B: Condensed Matter. 1997; 56(14): 8638–8650.

Lim SL, Tan KL, Kang ET. Langmuir. 1998; 14(18):5305–5313.

Lindfors T, Ivaska A. Journal of Electroanalytical Chemistry. 2002; 535(1-2):65–74.

Lis H, Sharon N. Annual Review of Biochemistry. 1986; 55:35–67.

Lis H, Sharon N. Chemical Reviews. 1998; 98(2):637–674. [PubMed: 11848911]

Loaiza OA, Lamas-Ardisana PJ, Jubete E, Ochoteco E, Loinaz I, Cabanero G, Garcia I, Penades S. Analytical Chemistry. 2011; 83(8):2987–2995. [PubMed: 21417434]

Loris R, Hamelryck T, Bouckaert J, Wyns L. Biochimica et Biophysica Acta. 1998; 1383(1):9–36. [PubMed: 9546043]

MacDiarmid AG, Chiang JC, Richter AF, Epstein A. Synthetic Metals. 1987; 18(1-3):285–290.

Manning DD, Bertozzi CR, Pohl NL, Rosen SD, Kiessling LL. The Journal of Organic Chemistry. 1995; 60(20):6254–6255.

Masters JG, Sun Y, Macdiarmid AG, Epstein AJ. Synthetic Metals. 1991; 41(1- 2):715–718.

Mayer M, Meyer B. Journal of American Chemical Society. 2001; 123(25):6108–6117.

Min W, Dunn AJ, Jones DH. The EMBO Journal. 1992; 11(4):1303–1307. [PubMed: 1563347]

Muilenberg, G. Handbook of X-ray Photoelectron Spectroscopy. PerkinElmer; NewYork: 1997.

Munoz EM, Correa J, Fernandez-Megia E, Riguera R. Journal of American Chemical Society. 2009; 131(49):17765–17767.

Murthy BN, Voelcker NH, Jayaraman N. Glycobiology. 2006; 16(9):822–832. [PubMed: 16782825]

Murthy BN, Zeile S, Nambiar M, Nussio MR, Gibson CT, Shapter JG, Jayaraman N, Voelcker NH. Rsc Advances. 2012; 2(4):1329–1333.

Nguyen TD, Camalet JL, Lacroix JC, Aeiyach S, Pham MC, Lacaze PC. Synthetic Metals. 1999; 102(1-3):1388–1389.

Otto K, Elwing H, Hermansson M. Journal of Bacteriology. 1999; 181(17):5210–5218. [PubMed: 10464189]

Pei YX, Yu H, Pei ZC, Theurer M, Ammer C, Andre S, Gabius HJ, Yan MD, Ramstrom O. Analytical Chemistry. 2007; 79(18):6897–6902. [PubMed: 17705448]

Plante OJ, Palmacci ER, Seeberger PH. Science. 2001; 291(5508):1523–1527. [PubMed: 11222853]

Pu KY, Shi JB, Wang LH, Cai LP, Wang GA, Liu B. Macromolecules. 2010; 43(23):9690–9697.

Ray A, Asturias GE, Kershner DL, Richter AF, Macdiarmid AG, Epstein AJ. Synthetic Metals. 1989a; 29(1):E141–E150.

Ray A, Richter AF, Macdiarmid AG, Epstein AJ. Synthetic Metals. 1989b; 29(1):E151–E156.

Ricard-Blum S, Peel LL, Ruggiero F, Freeman NJ. Analytical Biochemistry. 2006; 352(2):252–259. [PubMed: 16545768]

Sazou D. Synthetic Metals. 2001; 118(1-3):133–147.

Shaanan B, Lis H, Sharon N. Science. 1991; 254(5033):862–866. [PubMed: 1948067]

Sharon N, Lis H. Nature. 1986; 323(6085):203–204. [PubMed: 3762668]

Shen JF, Huang WS, Wu LP, Hu YZ, Ye MX. Composites Part A: Applied Science and Manufacturing. 2007a; 38(5):1331–1336.

Shen ZH, Huang MC, Xiao CD, Zhang Y, Zeng XQ, Wang PG. Analytical Chemistry. 2007b; 79(6): 2312–2319. [PubMed: 17295446]

Snauwaert P, Lazzaroni R, Riga J, Verbist JJ. Synthetic Metals. 1987; 18(1–3):335–340.

Solanki PR, Prabhakar N, Pandey MK, Malhotra BD. Journal of Molecular Recognition. 2008; 21(4): 217–223. [PubMed: 18446886]

Szunerits S, Niedziolka-Jonsson J, Boukherroub R, Woisel P, Baumann JS, Siriwardena A. Analytical Chemistry. 2010; 82(19):8203–8210. [PubMed: 20828205]

Tan KL, Tan BTG, Kang ET, Neoh KG. Physical Review B: Condensed Matter. 1989a; 39(11):8070–8073.

Tan KL, Tan BTG, Kang ET, Neoh KG. Physical Review B: Condensed Matter. 1989b; 39(11):8070–8073.

vanderSanden MCM. Synthetic Metals. 1997; 87(2):137–140.

Wei Y, Focke WW, Wnek GE, Ray A, Macdiarmid AG. The Journal of Physical Chemistry-Us. 1989; 93(1):495–499.

White RJ, Ervin EN, Yang T, Chen X, Daniel S, Cremer PS, White HS. Journal of American Chemical Society. 2007; 129(38):11766–11775.

Yavuz AG, Uygun A, Bhethanabotla VR. Carbohydrate Polymers. 2010; 81(3):712–719.

Yin X, Ding J, Zhang S, Kong J. Biosensors and Bioelectronics. 2006; 21(11):2184–2187. [PubMed: 16303298]

Yu XB, Xu DK, Cheng Q. Proteomics. 2006; 6(20):5493–5503. [PubMed: 16991201]

Yue J, Epstein AJ. Macromolecules. 1991; 24(15):4441–4445.

Yue J, Wang ZH, Cromack KR, Epstein AJ, MacDiarmid AG. Journal of American Chemical Society. 1991; 113(7):2665–2671.

Zand R, Agrawal BBL, Goldstein IJ. Proceedings of the National Academy of Sciences. 1971; 68(9): 2173–2176.

Zhou HJ, Lin YQ, Yu P, Su L, Mao LQ. Electrochemistry Communications. 2009; 11(5):965–968.

Zhou Y, Zheng KB, Grunwaldt JD, Fox T, Gu LL, Mo XL, Chen GR, Patzke GR. Journal of Physical Chemistry C. 2011; 115(4):1134–1142.

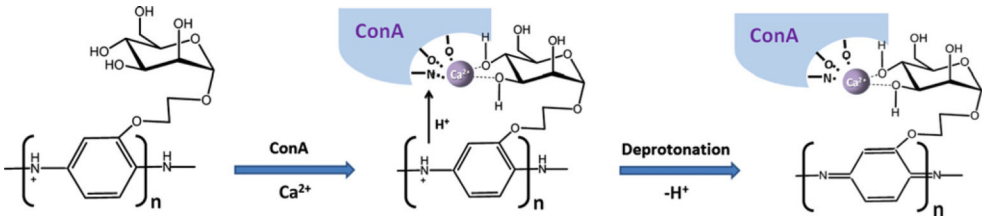

Scheme 1.
Deprotonation of mannosylated polyaniline (PANI) during the Con A binding.

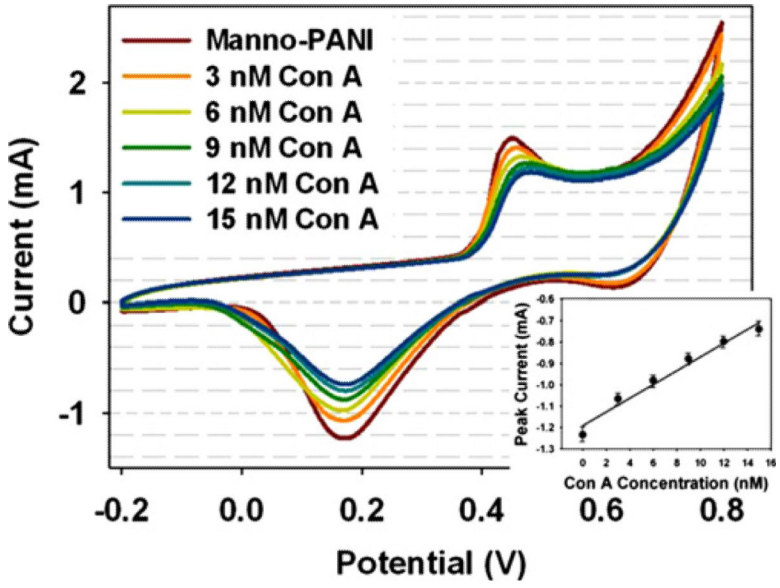

Fig. 1.

Cyclic voltammograms of manno-PANI film in the absence and presence of Con A at different concentrations in HEPES buffer with 2 mM Ca^{2+}. Scan rate was 50 mV/s, Ag/AgCl was used as a reference electrode, and Pt wire was used as a counter electrode.

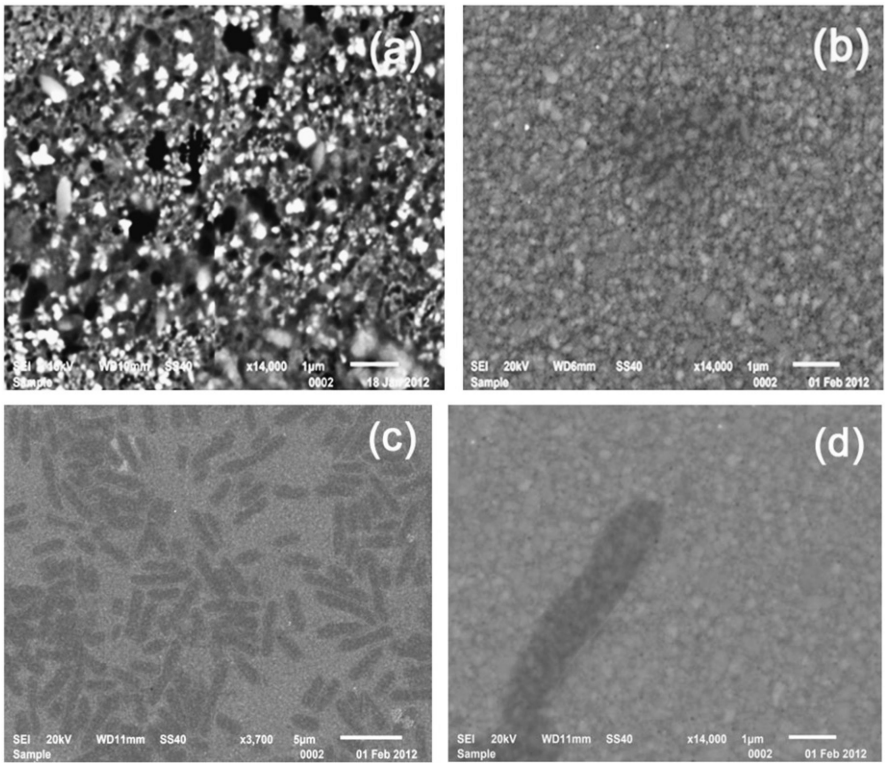

Fig. 2.

The SEM images of mannosylated polyaniline film on the ITO electrode in the absence (a) and presence (b) of 15 nM Con A, (c) and (d) in the presence of *Escherichia coli* after the experiment in (b).

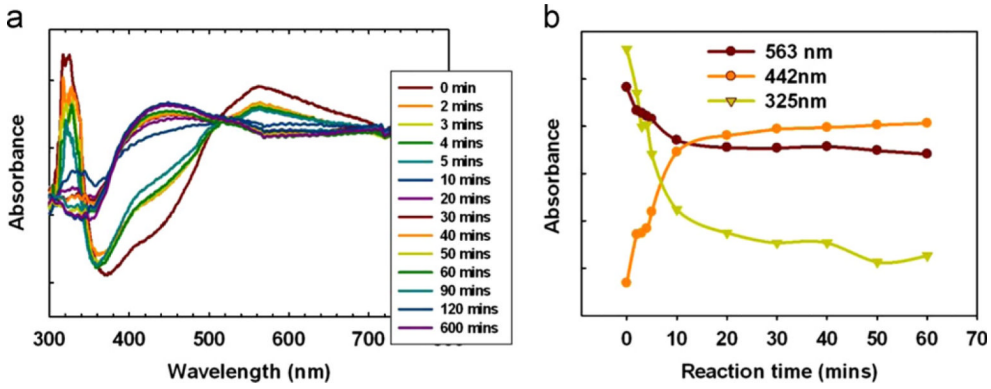

Fig. 3.

(a) UV–visible absorption spectra of manno-PANI on the ITO electrodes obtained for a period of time when 15 nM Con A was added. The ITO electrodes were washed with HEPES buffer each time before the measurement. (b) Correlation of absorbance vs. binding time of Con A to manno-PANI at 325 nm, 442 nm and 563 nm wavelength.

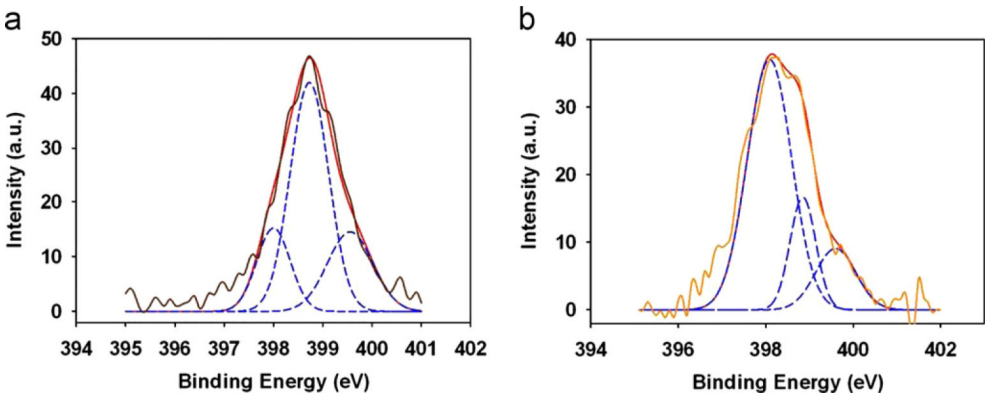

Fig. 4.

High-resolution N1s XPS core-level spectra of (a) manno-PANI and (b) after manno-PANI interaction with 15 nM Con A in HEPES. The brown solid lines are the XPS spectra and the red solid lines are for the total fits, blue dash lines are for the component fitted peaks for imine, amine and the radical cationic nitrogen atom. (For interpretation of the references to color in this figure legend, the reader is referred to the web version of this article.)

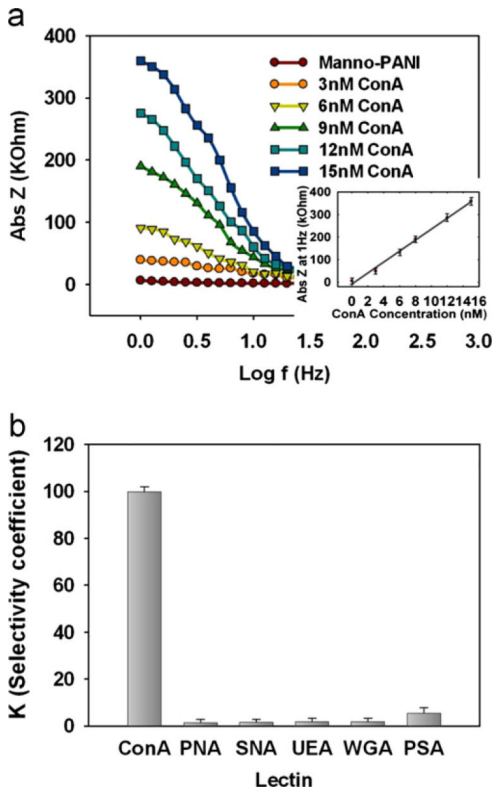

Fig. 5.

Quantification of manno-PANI and lectin interactions by electrochemical techniques for sensor application (a) EIS spectrum of manno-PANI film in the absence and presence of Con A at different concentrations Insert: Plot of impedance at 1 Hz vs. Con A concentration. (b) Comparison of the selectivity coefficients (K) for control lectins with respect to Con A at the same concentration (6 nM), where ΔZ is the difference of impedance of the manno-PANI film before and after the addition of a lectin and K=ΔZ (control lectin)/ΔZ (Con A).